Journal of Electron Spectroscopy and Related Phenomena 191 (2013) 65–70

Contents lists available at ScienceDirect

Journal of Electron Spectroscopy and Related Phenomena

journal homepage: www.elsevier.com/locate/elspec

Extracting detailed information from reflection electron energy loss spectra

Maarten Vos*

Atomic and Molecular Physics Laboratories, Research School of Physics and Engineering, The Australian National University, Canberra 0200, Australia

ARTICLE INFO

Article history:
Received 23 August 2013
Received in revised form 24 October 2013
Accepted 24 October 2013
Available online 6 November 2013

ABSTRACT

We use REELS (reflection electron energy loss spectroscopy) measurements at relatively large energies (up to 40 keV) and good energy resolution (0.3 eV) to extract the bulk and surface loss function for Au, Mo and Ta. For these cases there are small, but significant deviations between the electron-based estimates of the dielectric function as published by Werner et al. (J. Phys. Chem. Ref. Data 38 (2009) 1013), and the corresponding photon absorption/reflection based estimates. The present, higher-resolution electron-based measurements reveal more of the fine structure in the differential inverse inelastic mean free path (DIIMFP) and the differential surface excitation probability (DSEP). The same fine-structure is visible in the photon-derived estimates of the bulk and surface loss function, quantities closely related to the DIIMFP and DSEP. Thus we demonstrate that it is indeed possible to derive these fine details of the surface and bulk loss function with REELS, underlining its potential for extracting information on the dielectric function of materials.

1. Introduction

The relation between electron energy loss spectra (EELS) and the dielectric function has been well established for a long time. Transmission EELS measurement at high energies (≈50 keV) were used more than 40 years ago to derive the dielectric function, based on the measured loss function (see Ref. [1] for a review), sometimes with exquisite energy resolution (≈100 meV) [2]. In these experiments multiple scattering could be constrained to manageable levels by the use of thin, self-supporting films, and surface excitations were minor at these energies and could be further reduced by going slightly off-axis. The loss function measured in this way can be used to derive the dielectric function of the material, important not only for the interaction of light with matter [3], but also as the basis for an accurate determination of the inelastic mean free path of electrons in matter [4].

Later (1980–2000) the interest shifted to lower energy experiments (≈1 keV), as understanding of inelastic and elastic processes at these energies was required in the context of X-ray Photoelectron Spectroscopy (XPS), which was being developed into one of the major tools of surface science. Transmission experiments were not possible at these low energies, and reflection electron energy loss spectroscopy (REELS) became an important technique to study the underlying processes that contributes to the shape (in particular the shape of the 'background') of an XPS spectrum.

Initially it was hard to extract information about the dielectric function directly from REELS spectra, as untangling the effects of multiple scattering and surface excitations was more complex in this case, but slowly the mathematical techniques were developed to analyse these spectra in terms of either an effective energy loss function [5,6], or in terms of a bulk and surface loss functions [7,8]. This increased understanding has renewed the interest into extracting the dielectric function from electron scattering results, but now in a reflection geometry. This is an attractive option, not requiring thin self-supporting samples (as transmission EELS) and making it possible to determine the dielectric function from thin, nano-scale overlayers. The results so far were recently summarised by Werner et al. [9].

In our laboratory we conduct electron scattering experiments at relatively high energies (5–40 keV) and good energy resolution (0.3 eV). The high energies allow us to explore the electronic structure (i.e. dielectric function) of relatively thick layers [10,11]. Further, for a large-angle (backward) scattering geometry the recoil energy transferred by the energetic electron while scattering elastically from an atom is easily resolved, allowing for the determination of the mass of the scatterer (and hence surface layer composition). The resulting combination of the recoil losses and REELS spectra is a very versatile tool for the study of relatively thick layers (10–100 nm) (see e.g. Ref. [12]). In this paper we focus on the REELS spectra obtained with this spectrometer, and compare the results acquired under these conditions with those from the compilation of Werner et al. [9], to see how their assertion that REELS can be used effectively to determine the dielectric function holds up. For this we focus on three cases (Au, Mo and Ta) where there are differences in

* Tel.: +61 2 6125 4985.
E-mail address: maarten.vos@anu.edu.au

0368-2048/$ – see front matter © 2013 Elsevier B.V. All rights reserved.
http://dx.doi.org/10.1016/j.elspec.2013.10.007

certain features of the loss functions between the results shown in Ref. [9] and results published elsewhere.

2. REELS and dielectric functions

We follow closely the methods developed by Werner [7,8] and as these have been covered extensively elsewhere, we will only highlight a few important points here.

There are several approximations behind Werner's algorithm. First, it is assumed that there are only two different kind of excitations in the REELS spectra (surface and bulk) that can be described with two energy loss probability density functions. Furthermore, surface excitations along the incoming and outgoing trajectories are assumed to be independent from each other and from bulk losses.

The next assumption, behind Werner's algorithm, is that the probability density functions for bulk and for surface excitations are independent from the energy and geometry. It is then possible to separate bulk and surface loss function if two measurements are available for which the ratio of surface and bulk excitations differ significantly. Maximising this difference will result in a more accurate decomposition of surface and bulk loss function. Consider the REELS spectrum Y plotted as a function of the energy loss ω and with the elastic peak normalised to unit area. $Y(\omega)$ can then be written as [8,9]:

$$Y(\omega) = \sum_{n_b=0}^{\infty} \sum_{n_s=0}^{\infty} A_{n_b,n_s} \Gamma_{n_b} \otimes \Gamma_{n_s} \tag{1}$$

with A_{n_b,n_s} the frequency that trajectories with n_b bulk losses and n_s surface losses occur. Γ_{n_b} (Γ_{n_s}) is the $n_b - 1$ ($n_s - 1$) self convolution of the normalised loss function w_b (w_s).

It is assumed that bulk and surface excitations are independent i.e. $A_{n_b,n_s} = A_{n_b} \times A_{n_s}$ with A_{n_b} and A_{n_s} the bulk and surface partial intensities normalised such that $A_{n_b=0} = A_{n_s=0} = 1$. A_{n_b} can be obtained from Monte Carlo simulations, and is determined mainly by the elastic scattering properties of the system (with a minor dependence on the inelastic mean free path). For each surface crossing the probability P_s that a surface excitations is created is taken from the formula suggested by Chen [13]:

$$P_s = \frac{1}{\cos\theta} \frac{2.896}{\sqrt{E_0}}. \tag{2}$$

from which A_{n_s} can be obtained. We then use the procedure described in the appendix of Ref. [8] to solve Eq. (1) for w_b and w_s, based on two spectra taken under conditions where the contribution of surface excitations differ.

The bulk differential inverse inelastic mean free path (DIIMFP) W_b can be expressed in terms of the bulk dielectric constant $\varepsilon(q,\omega)$ (see e.g. Ref. [14]):

$$W_b(\omega, E_0) = \frac{1}{\pi a_0 E_0} \int_{q_-}^{q_+} \frac{dq}{q} \mathrm{Im} \frac{-1}{\varepsilon(q,\omega)}. \tag{3}$$

Here E_0 is the incoming energy, a_0 the Bohr radius and $\boldsymbol{q}$ is the difference between the momentum of the probing electron before and after the collision: $\boldsymbol{q} = \boldsymbol{k}_1 - \boldsymbol{k}_0$. The limits of the integration are given by: $q_- = \sqrt{2mE_0} - \sqrt{2m(E_0-\omega)}$, and $q_+ = \sqrt{2mE_0} + \sqrt{2m(E_0-\omega)}$ i.e. the integration is over all possible magnitudes of q. The main contributions (due to the $1/q$ factor in Eq. (3)) are from small q values. The smallest q value one can reach (q_-) is in the forward direction, but this lower limit is not zero as, due to the energy loss, $|k_1| < |k_0|$. The value of q_- decreases with increasing E_0 values.

The area of W_b is equal to $1/\lambda$ with λ the inelastic mean free path. Multiplying W_b by λ we obtain the normalised loss function w_b. In Fig. 1 we plot w_b for E_0 values as indicated. Here we use the model dielectric function of Ta as given in Ref. [9] and the SESINIPAC package of Novák [15,16] to evaluate Eq. (3). The loss structures appear somewhat more pronounced for larger E_0 values, presumably because the integration for larger E_0 extends to smaller q-values. This results in the shape of w_b approaching the shape of $\mathrm{Im}(-1/\epsilon(0,\omega))$ more and more with increasing E_0 values, as is illustrated in Fig. 1. It is $\mathrm{Im}(-1/\epsilon(0,\omega))$ that is probed in photon-based experiments. Thus the approximation that the shape of w_b is not energy dependent is not perfect, and how this error propagates in the calculation of w_s and w_b, especially if the difference in contributions due to surface excitations between both experimental conditions are only minor, is not clear.

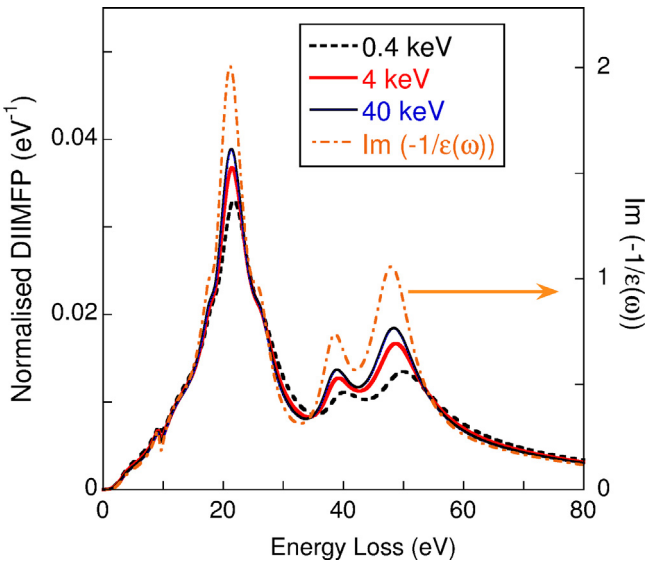

Fig. 1. Normalised DIIMFP w_b, as calculated for Ta based on a model dielectric function, for the incoming electron energies as indicated. With increasing E_0 the shape starts resembling $\mathrm{Im}(-1/\epsilon(0,\omega))$ more closely.

Another important quantity is W_s: the differential surface excitation parameter (DSEP). It represents the change in the energy loss processes due to the presence of the surface. There are two contributions to W_s as pointed out by Ritchie [17]. Excitations only possible at the surface, due to its reduced symmetry, and a reduction in the probability of exciting bulk excitations in the near surface region (often referred to as 'begrenzung effect'). The first contribution is proportional to $\mathrm{Im}(-1/(\epsilon+1))$, the second proportional to W_b and it may cause W_s to go slightly negative for ω values where W_b is strongly peaked. The DSEP scales approximately as $\sqrt{1/E_0}$ (see Eq. (2)). The DSEP normalised to unit area is indicated by w_s, and this quantity should be fairly independent of incoming energy and the angle of the surface crossing.

3. Some details

3.1. Experimental details

Our spectrometer has two electron guns and one analyser. The scattering angle is either 45° or 135° and the surface normal of the sample, incoming and outgoing beam are all in one plane. Both guns have a BaO cathode for small energy spread. The main (positive) high voltage is applied to the sample, while the gun cathode is held at a small negative voltage (−500 V for a 40 keV beam, −62.5 V for a 5 keV beam). In this way the ripple on the main high voltage (up to 39.5 kV) does not contribute to the energy resolution. The beam current is of the order of 1 nA for measurements with

E_0 = 40 keV, an order of magnitude less for 5 keV measurements. The beam current is measured, with a meter floating at the high voltage, and a pulse train is created with a frequency proportional to the beam current. This pulse train is transmitted to ground potential via fiber optics. The measurement at a certain gun-analyser offset voltage is stopped when a predetermined charge amount has been accumulated.

Samples are sputter-cleaned using either Ar^+ or Xe^+ ions. In the case of Au a fresh surface was also prepared by evaporating 10–20 nm Au on a previously cleaned surface.

3.2. Monte Carlo Simulation

A Monte Carlo simulation program was written following fairly close the approach described in Ref. [14]. The somewhat special property of this program is that it keeps track of the recoil losses, but this is of no importance here. Basically the electrons are followed through the crystal and elastic scattering events are modelled using the elastic scattering cross section as derived from the ELSEPA package of Salvat and coworkers [18]. The simulation is stopped when the trajectory either leaves the crystal again, or is longer than 10 times the inelastic mean free path. For those trajectories that leave the crystal with the electron moving towards the analyser we determine from its path length L the chance that it contributes to events with n_b = 0, 1, 2, ... inelastic events. This is given by a Poisson distribution:

$$P(n_b) = \left(\frac{L}{\lambda}\right)^{n_b} \frac{e^{-L/\lambda}}{n_b!} \quad (4)$$

From the simulation of a large number of trajectories we obtain the partial intensity distribution A_{n_b}, where A_0 is normalised to 1.

4. Results

4.1. Au

We focus first our attention on Au. Here it is quite well established that the surface plasmon should be at an energy loss near 2.5–2.7 eV and it stands out clearly in low energy REELS measurements [20,21]. In the compilation of Werner et al. the surface loss function has a peak at energies of 3.25 eV [9]. This loss feature was only resolved after deconvolution [22]. Our spectrometer resolves the loss feature directly. We choose 2 configurations to maximise the difference in surface sensitivity: geometry (I) glancing in/out (67.5° away from the surface normal) at 5 keV and (II) perpendicular in, 45° out at 40 keV. The resulting spectra are shown in Fig. 2(A). The difference in surface sensitivity between the two configurations used is much larger than in an earlier study [23], making the extraction of the surface loss function even more straight forward. The elastic peaks are always aligned with zero energy loss (i.e. we neglect the recoil loss) and normalised to unit area. The spectra had a minimum near 1 eV. The Au elastic peak was removed by simply replacing the intensity between 0 and 1 eV with a straight line starting at 0 at 0 eV and equal to the observed intensity at 1 eV. The spectrum has a pronounced maximum in geometry (I) near 2.57 eV. In geometry (II) there is a less pronounced peak at a very similar energy loss value.

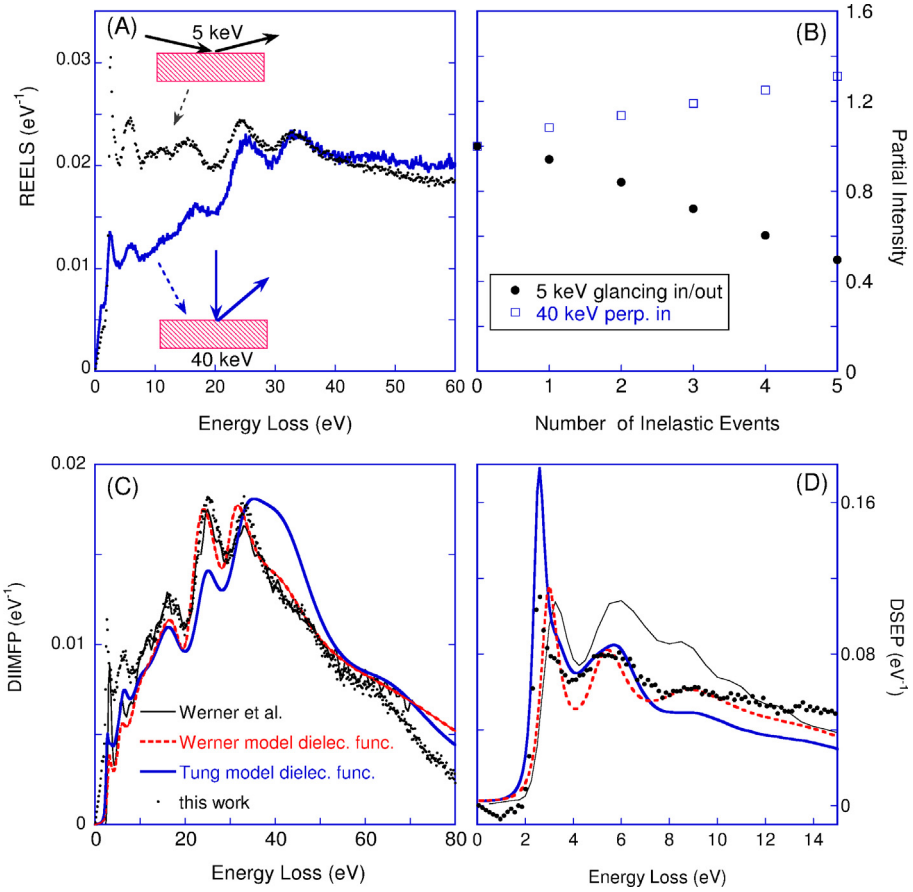

Fig. 2. REELS spectra taken at different energies and geometries for Au (A) and the partial intensities as obtained from a Monte Carlo simulation (B). In (C) and (D) we show the DIIMFP and DSEP obtained from these measurements in combination with the partial intensities obtained from the Monte Carlo simulations. The obtained DIIMFP and DSEP are compared with results from other experiments [9] and model dielectric functions [9,19].

Fig. 2(B) shows the bulk partial intensities as obtained with the Monte Carlo code. These are used as input for the 'simple deconvolution procedure' as described in Ref. [8], and the resulting (normalised) DIIMFP and DSEP are shown in Fig. 2(C) and (D). Due to the large difference in surface sensitivity of both geometries, both the obtained DSEP and DIIMFP are relatively free of noise and show a wealth of structure. For energy losses above 10 eV there is excellent agreement between the DIIMFP of Ref. [9] and the current measurement. The agreement for the DSEP is somewhat less good. There is indeed a difference in position of the maximum of the DSEP, which is now in better agreement with the expected value for a Au surface plasmon. Also, the intensity in the region for $6\,eV < \omega < 10\,eV$ is less in the current DSEP. It is interesting to compare our DIIMFP and DSEP with that obtained, using SESINIPAC, from the model dielectric function as published by Tung et al. [19] and Werner et al. [9]. The dielectric function of Werner describes our observed DIIMFP very well for ω values over 20 eV, but has somewhat too small an intensity at lower ω values. This good agreement is not too surprising as the dielectric function was modelled based mainly on the (very similar to our) DIIMFP obtained from his REELS data. The model dielectric function of Tung et al., based on both REELS [24] and optical data [3], has too much intensity for ω near 42 eV. This reflects the difference in the values for $\mathrm{Im}(-1/(\epsilon(0, \omega)))$ obtained from optical and REELS data [9].

The DSEP obtained in this work is in better agreement with the DSEP calculated from either model dielectric function than the experimental DSEP of Ref. [9]. The model dielectric function of Werner et al. was based on a weighted fit of the DIIMFP and DSEP of Ref. [9]. It is thus, at first sight, surprising that the DSEP obtained from this model dielectric function agrees better with our new measurement, than the DSEP of the measurement set from which the dielectric function was derived. Except for the position of the first maximum, the calculated DSEP from Ref. [9] describes the current result very well. The better agreement with the new measurement is a consequence of the fact that the DSEP and DIIMFP are linked (they are derived from a single dielectric function) but the DSEP is harder to obtain experimentally. When the DIIMFP is determined with greater precision than the DSEP then the DSEP derived from a dielectric function, based on this measurement, will be more precise than the directly measured DSEP. The DSEP obtained from the work of Tung et al. [19] agrees in the position of the maximum, but the calculated intensity at the maximum is larger than the one observed here.

4.2. Mo

The next case study we want to discuss is molybdenum. The shape of $\mathrm{Im}(-1/(\epsilon+1))$, as obtained by Weaver et al. [25], showed two peaks with a plateau in between. The DSEP of Werner et al. [9] has a more triangular shape with a hint of a shoulder at the high energy side.

We measured Mo after cleaning by ion sputtering using a scattering angle of 45°, and an incoming and outgoing beam at an angle with the surface normal of 67.5°. There are two pronounced peaks in the energy loss spectrum, one near 10 eV and one near 25 eV with a plateau in between (with a hint of a very small peak near 16 eV) (Fig. 3, top panel). The exact shapes of both peaks are slightly different though, most noticeably the 5 keV spectrum has a clear shoulder at the low-energy loss side of the main peak.

Using the 5 and 40 keV spectrum to separate out the DIIMFP and DSEP, in the same way as described for Au, we get estimates that resemble that of the photon based loss function [25] very well. As is clear from Fig. 3, central panel, the main peak is at slightly larger energy loss (by 0.5 eV) in the present work and near 35 eV the present results are, just like the results from Ref. [9], considerable lower in intensity than the loss function of Weaver et al. [25].

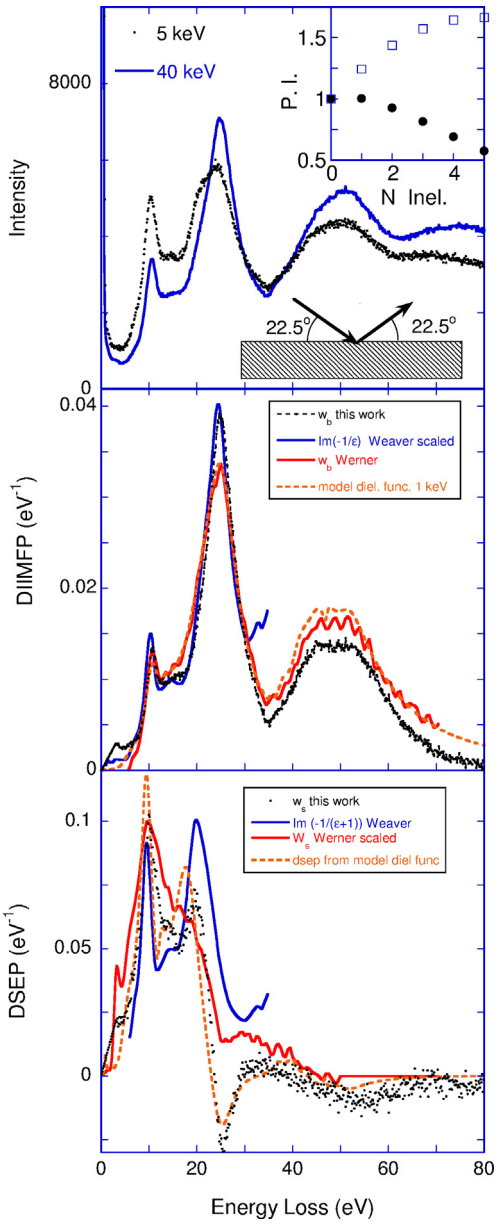

Fig. 3. REELS spectra of Mo taken at two different energies (top panel). The inset shows the partial intensities obtained from the Monte Carlo procedure for this case. The central panel shows the normalised DIIMFP w_b as obtained from the data analysis procedure. It is compared to earlier electron based measurement of w_b [9] as well as $\mathrm{Im}(-1/\epsilon)$ as obtained from synchrotron data [25]. It is also compared to w_b as calculated based on a model dielectric function [9]. The bottom panel shows a similar comparison for the DSEP (w_s).

The present surface loss function (Fig. 3, lower panel) has clearly two peaks, just as suggested by $\mathrm{Im}(-1/(\epsilon+1))$ shape obtained by Weaver [25]. The peak at higher energy loss is in the present work less intense than the first peak, whereas in Weaver's data it is the other way around. Clearly in the electron-based DSEP the second peak is affected by the reduction in the bulk plasmon creation rate near the surface, which is the cause of the negative intensity at slightly larger losses. The DSEP as calculated using Werner's model dielectric function again fits the present DSEP much better than the DSEP of his own experimental work, including the negative intensity near 26 eV [9]. As discussed before, this better agreement of the DSEP is indicative of a higher level of internal consistency of the present results.

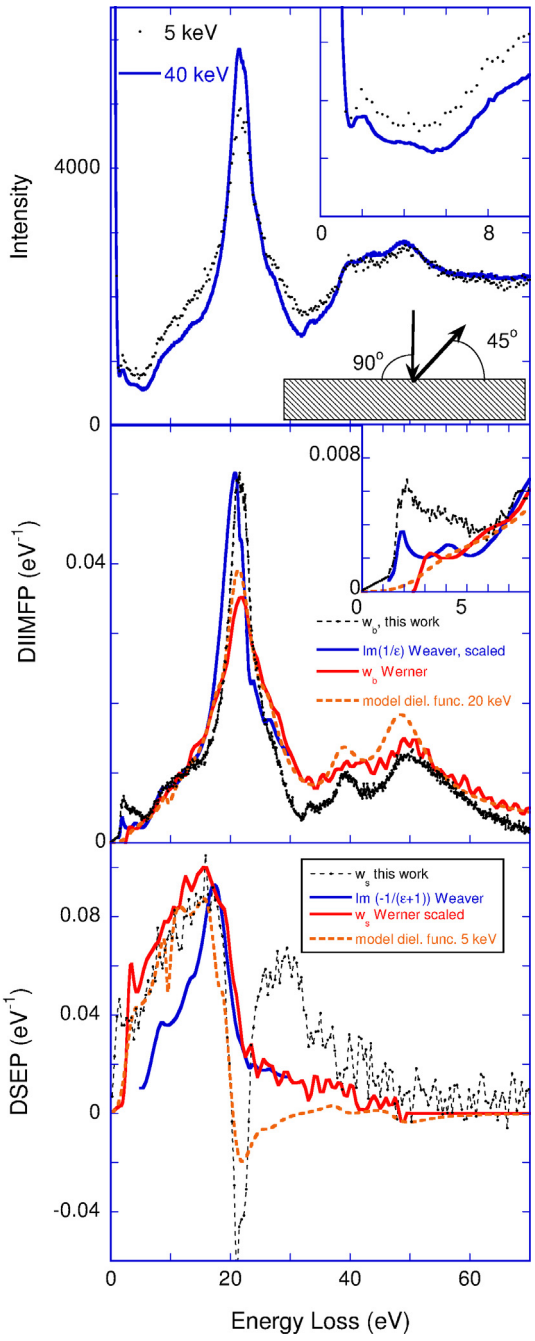

Fig. 4. Same as Fig. 3, but now for Ta. The inset now shows a magnification of the low loss region.

4.3. Ta

Tantalum is interesting in this context as the X-ray based data from Weaver et al. [25] show a clear peak at 2 eV [25], even a smaller energy loss than the surface plasmon peak of Au. This peak is completely missing in the analysis of Werner [9]. Is it possible to resolve this peak by electron scattering? Indeed, already in the raw data we see a small peak at this energy just adjacent to the elastic peak, see Fig. 4 top panel. Both spectra were taken with the incoming beam along the surface normal, a bulk sensitive geometry, and the feature near 2.0 eV is of comparable strength for incoming energies of 5 keV and 40 keV. This clearly indicates that this feature is indeed part of the bulk loss function. This peak is followed by a second, even weaker peak near 4 eV which is also visible in the X-ray based estimate of the loss function.

We should add a word of caution here. In this geometry the recoil of atoms are resolved at 40 keV. For example oxygen, present on the surface would give rise to a peak at 4.4 eV energy loss relative to the Ta elastic peak. Indeed a peak near 4.4 eV is seen before surface-cleaning of Ta metal and even stronger for Ta_2O_5 films [12]. It was our desire to understand our recoil data better that prompted us to look at the clean Ta metal spectrum more closely, and see if the extra bumps at 2 and 4 eV (corresponding to approximately mass 40 and 20 respectively, when interpreting these features as the elastic peak of impurities) were due to contamination or not. The fact that these bumps did not change noticeably after additional sputter and annealing treatments *and* their presence in the X-ray derived loss function treatments made it clear that they are intrinsic to the Ta metal.

The Ta bulk and surface loss function were derived as described before. As the surface loss contribution was small for both measurement geometries used, we cannot expect a very accurate determination of the DSEP, but the bulk loss function should be reliable. The maximum intensity of the DIIMFP is near 21.5 eV, almost 1 eV larger value than the maximum of the loss function of Weaver et al. [25], but in good agreement with the electron scattering result of Werner et al. [9]. There is another small but distinct peak at 33 eV. There are hints of this feature in the density functional theory derived loss function of Ref. [9] as well as in the calculations of Ref. [26]. The features near 40 eV and 50 eV are clearly seen in these data more so than in loss function determined at lower E_0 values, but compare well with the results of the DIIMFP calculated based on the loss function of Ref. [9]. This is in-line with the expectation that these features should be more pronounced at higher probing energies (see Fig. 1). The features observed between 2 and 50 eV in the DIIMFP all are corroborated by other measurements and/or theory. The shape of the spectrum in the low-loss region resembles the loss function of Weaver et al. [25], but the intensity is somewhat higher. This is probably rooted in the way we subtracted the elastic peak. The DSEP obtained from these measurements is clearly of less quality, as both geometries used are rather bulk sensitive. It resembles the DSEP of the model dielectric function [9] more than $\mathrm{Im}(-1/(\varepsilon+1))$ of Weaver et al. [25] but this measurement geometry is clearly much more suitable for extracting the DIIMFP than the DSEP.

5. Discussion and conclusion

We investigated the DSEP and DIIMFP for several cases where there were unexpected differences between, in particular, the DSEP, and previous determinations of $\mathrm{Im}(-1/(\epsilon+1))$. In all cases the more precise measurements described here went a long way to clarify the situation. Overall these results are very encouraging for the prospect of obtaining high-quality information about the dielectric function from REELS data, and seem to validate the data analysis framework used. In particular we showed that, with good energy resolution, one can resolve weak features only 2 eV away from the very intense elastic peak. Also the use of higher energy makes it possible to probe closer to zero momentum transfer, increasing the structure for some levels. If this energy-dependence of the DIIMFP requires modification of the analysis procedure, in order to achieve quantitative reliable estimates of the dielectric function remains to be investigated. An energy-dependence of the DIIMFP and the DSEP was also noted in the work of Calliari et al. in the context of the analysis of REELS spectra at considerable lower energy [27].

Problems with changes in the DIIMFP with energy can be avoided in principle if one measures at only one energy, and obtains

the surface and bulk loss function by comparing the results of a bulk-sensitive and a surface sensitive geometry. In that case one relies on the accuracy of the angular dependence of the surface excitation probability (Eq. (2)).

The paper shows that high-energy measurements can provide high quality information about the DIIMFP and DSEP, especially if care is taken that at least the lower-energy measurement is in a surface-sensitive geometry. The geometries used in the Au measurement (scattering over 45° at 5 keV and 135° at 40 keV) is particularly suitable, as here the high energy measurement is affected by surface excitation in only a minor way. The geometry of the Mo experiment (scattering over 45° at 5 keV and at 40 keV) is a good compromise if only one scattering angle can be employed. Finally the geometry of the Ta measurement (scattering over 135° at 5 keV and at 40 keV) is suitable for the determination of the DIIMFP, but provides only limited information about the DSEP.

A logical next step, not pursuit here, is to investigate if we can improve on the model dielectric functions in the literature. This is a complicated question as a proper description is not obtained by just adjusting the coefficients, but also requires better understanding of the accuracy of the w_s and w_b functions obtained (e.g. understanding the consequences of the energy dependence of w_b, see Fig. 1), as well as a better understanding of the dispersion of the levels. For a discussion of the different possibilities here see the recent work of Denton et al. [28] or Bourke and Chantler [29].

Acknowledgements

This work was made possible by a grant of the Australian Research Council. The author want to thank Pedro Grande and Erich Weigold for critically reading the manuscript.

References

[1] J. Daniels, C. von Festenberg, H. Raether, K. Zeppenfeld, Springer Tracts Mod. Phys. 54 (1970) 77–135.
[2] J. Daniels, Z. Phys. 203 (1967) 235–249.
[3] E. Palik, Handbook of Optical Constants of Solids II, Academic Press, New York, 1991.
[4] D. Penn, Phys. Rev. B 35 (1987) 482–486.
[5] S. Tougaard, I. Chorkendorff, Phys. Rev. B 35 (1987) 6570–6577.
[6] S. Tougaard, F. Yubero, Surf. Interface Anal. 36 (2004) 824–827.
[7] W.S. Werner, Surf. Sci. 588 (2005) 26–40.
[8] W. Werner, Surf. Sci. 604 (2010) 290–299.
[9] W. Werner, K. Glantschnig, C. Ambrosch-Draxl, J. Phys. Chem. Ref. Data 38 (2009) 1013–1092.
[10] M. Vos, M. Went, Surf. Sci. 601 (2007) 4862–4872.
[11] M. Vos, M. Went, J. Electron Spectrosc. Relat. Phenom. 162 (2008) 1.
[12] M. Vos, P. Grande, S. Nandi, D. Venkatchalam, R. Elliman, J. Appl. Phys. 114 (2013) 073508.
[13] Y.F. Chen, Surf. Sci. 519 (2002) 115–124.
[14] W.S.M. Werner, Surf. Interface Anal. 31 (2001) 141.
[15] N. Pauly, M. Novák, A. Dubus, S. Tougaard, Surf. Interface Anal. 44 (2012) 1147–1150.
[16] N. Pauly, M. Novák, S. Tougaard, Surf. Interface Anal. 45 (2013) 811–816.
[17] R.H. Ritchie, Phys. Rev. 106 (1957) 874–881.
[18] F. Salvat, A. Jablonski, C.J. Powell, Comput. Phys. Commun. 165 (2005) 157–190.
[19] C. Tung, Y. Chen, C. Kwei, T. Chou, Phys. Rev. B 49 (1994) 16684–16693.
[20] A. Pulisciano, S.J. Park, R.E. Palmer, Appl. Phys. Lett. 93 (2008) 213109.
[21] A. Politano, V. Formoso, G. Chiarello, Plasmonics 3 (4) (2008) 165–170.
[22] S. Hummel, A. Gross, W.S.M. Werner, Surf. Interface Anal. 41 (2009) 357–360.
[23] W. Werner, M.R. Went, M. Vos, Surf. Sci. 601 (2007) L109–L113.
[24] S. Tougaard, J. Kraaer, Phys. Rev. B 43 (1991) 1651–1661.
[25] J. Weaver, D. Lynch, C. Olson, Phys. Rev. B 10 (1974) 501–516.
[26] P. Romaniello, P. de Boeij, F. Carbone, D. van der Marel, Phys. Rev. B 73 (2006) 075115.
[27] L. Calliari, M. Filippi, A. Varfolomeev, Surf. Sci. 605 (2011) 1568–1576.
[28] C.D. Denton, R.S. Abril, I. Garcia-Molina, J.C. Moreno-Marín, S. Heredia-Avalos, Surf. Interface Anal. 40 (2008) 1481–1487.
[29] J.D. Bourke, C.T. Chantler, J. Phys. Chem. A 116 (2012) 3202–3205.